Fabrication of polyethyleneimine-functionalized reduced graphene oxide-hemin-bovine serum albumin (PEI-rGO-hemin-BSA) nanocomposites as peroxidase mimetics for the detection of multiple metabolites

Xiaoyue Zhang, You Yu, Jinglin Shen, Wei Qi[*], Hua Wang[**]

Institute of Medicine and Materials Applied Technologies, College of Chemistry and Chemical Engineering, Qufu Normal University, Qufu Shandong, 273165, China

HIGHLIGHTS

- PEI-rGO-Hemin-BSA nanocomposites were fabricated via π-π interactions.
- The PEI-rGO-Hemin-BSA demonstrated high peroxidase-like catalytic activity.
- The PEI-rGO-Hemin-BSA can combine further with an oxidase to detect its substrate.
- Glucose, cholesterol, L-lactate, and choline were detected sensitively and easily.
- The strategy could find an application in multiple metabolites detection.

GRAPHICAL ABSTRACT
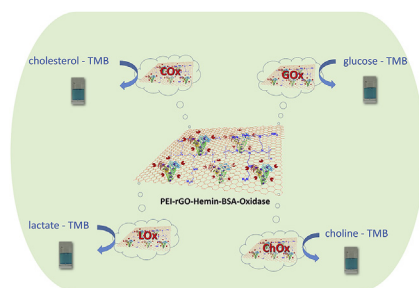
ABSTRACT

The ultrasensitive bioassays are increasingly demanded for disease diagnosis and environmental monitoring. The combined unique natures of the components in nanocomposites have led to their wide applications in bioanalysis. In the current study, a simple strategy for preparing polyethyleneimine-functionalized reduced graphene oxide-hemin-bovine serum albumin (PEI-rGO-Hemin-BSA) nano-composites as peroxidase mimetics was demonstrated. The developed nanocomposites of PEI-rGO-Hemin-BSA showed an excellent peroxidase-like activity. Importantly, through the glutaradelhyde crosslinking, PEI-rGO-Hemin-BSA could be further simply combined with various oxidases such as glucose oxidase, cholesterol oxidase, lactate oxidase and choline oxidase for the detection and quanti-tative measurement of multiple metabolites including glucose, cholesterol, L-lactate, and choline. The developed detection strategy, which is sensitive, convenient, low-costed, and in tiny sample consump-tion, could be expected wide applications in the disease diagnosis and management of metabolite disorders.

© 2019 Elsevier B.V. All rights reserved.

1. Introduction

Quantitative measurement or monitoring of small molecule metabolites in blood or other biological samples, such as glucose,

cholesterol, and lactate, is of central importance in diagnosis and healthcare. To accurately evaluate metabolite levels, investigation of multiple metabolites is necessary [1–5]. However, for most of the current methods, this is limited by the requirement of a large amount of samples, different assays, special instruments, long waiting time and high cost [6,7]. In this work, a new type of peroxidase mimetic nanocomposites was developed for the measurement of multiple metabolites in samples, which is sensitive, prepared easily, low-costed, and in tiny sample consumption.

Natural enzymes are well known because of their high specificity and high catalytic efficiency under mild conditions [8], however, their practical applications have been restricted significantly due to their properties such as high cost of preparation, purification and storage, low stability caused by denaturation and digestion, and sensitivity of catalytic activity to environmental conditions [9,10]. Therefore, the development of cheap, stable and efficient artificial enzyme mimics has become an increasingly important focus for researchers in the past few decades.

In the field of artificial enzymes, nanoenzymes, i.e. nanomaterials showing enzyme-like catalytic activities, have attracted enormous interest due to their convenient preparation and storage, excellent chemical stability, feasible surface modification, low cost of production and high flexibility in composition, size, shape control [11–14]. Particularly, a large variety of nanoenzymes including magnetic nanomaterials [15–17], metal oxide nanoparticles [18–21], metal nanoparticles [22–25], metal nanoclusters [26–29], carbon nanomaterials [30–34], and nanocomposites [35–41] have shown peroxidase-like catalytic activities since the first nanoparticle-based artificial enzyme, Fe_3O_4 nanoparticle, was reported to possess an enzyme activity similar to natural peroxidase [42]. For example, the peroxidase-like artificial enzyme based on hemin is one of them [43–50].

Hemin, iron protoporphyrin, is the active center of hemeprotein family including cytochromes, peroxidase, myoglobins and hemoglobins, and it has similar catalytic activity as that of the peroxidase enzyme [44,45]. However, there are challenges for the direct application of hemin because of its low catalytic activity caused by its poor aqueous solubility and high tendency to form inactive dimers [46]. Therefore, the design of hem-containing artificial peroxidase has become an increasingly important topic [47,48]. Our group has previously reported hemin-bovine serum albumin (Hemin-BSA) composites as peroxidase-like enzymes displaying high catalytic activity in the typical redox reaction of TMB and H_2O_2 [49,50]. Based on these work, in the present study, the hemin-BSA composites will be combined with polyethyleneimine-functionalized reduced graphene oxide (PEI-rGO) to obtain a new type of nanocomposites with peroxidase-like catalytic activities, as shown in Scheme 1. Polyethyleneimine (PEI), a water-soluble polymer, can easily react with the materials containing carboxyl or epoxy groups due to its active amine groups. Therefore, PEI is an ideal candidate for the modification of graphene to prevent its aggregation and extend its further application [51,52].

Moreover, as shown in Scheme 1, using glutaraldehyde (GA) as a crosslinker, the obtained PEI-rGO-Hemin-BSA can further bine with an oxidase such as glucose oxidase (GOx), cholesterol oxidase (COx), lactate oxidase (LOx) and choline oxidase (ChOx). The as-developed PEI-rGO-Hemin-BSA-GOx, PEI-rGO-Hemin-BSA-COx, PEI-rGO-Hemin-BSA-LOx, and PEI-rGO-Hemin-BSA-ChOx can detect metabolites including glucose, cholesterol, lactate, and choline, respectively. Thus, a simple strategy of detecting multiple metabolites is proposed, which could be expected to find use in diagnosis and management of metabolic disorders and the associated diseases.

2. Experimental

2.1. Reagents and apparatus

Glucose oxidase from Aspergillus niger, cholesterol oxidase from microorganisms, lactate oxidase from Aerococcus viridans, choline oxidase from Alcaligenes sp., Hemin from bovine blood, N-(3-Dimethylaminopropyl)-N′-ethylcarbodiimide hydrochloride (EDC hy-drochloride), ascorbic acid (AA), dopamine (DA), uric acid (UA), glucose, bovine serum albumin (BSA), cholesterol, choline, lactate
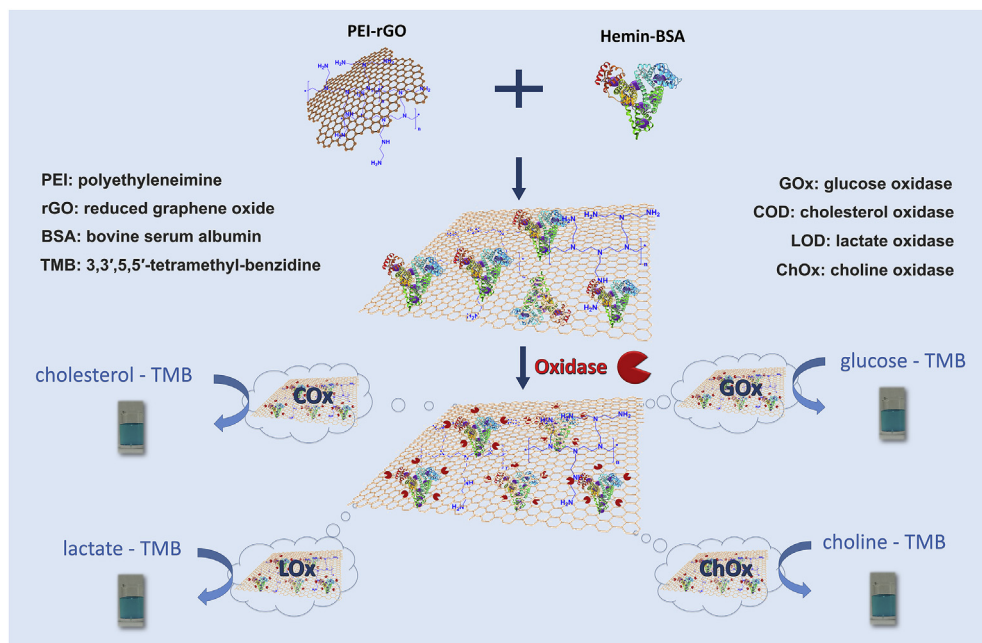
Scheme 1. Schematic representation of the fabrication of polyethyleneimine-functionalized reduced graphene oxide-hemin-bovine serum albumin (PEI-rGO-Hemin-BSA) nanocomposites as peroxidase mimetics for metabolites detection.

and N-Hydroxysuccinimide (NHS) were purchased from Sigma-Aldrich (USA). Expandable graphite (EG) 8099200 was purchased from Qingdao BCSM. Co., Ltd. (China). Dimethyl sulfoxide (DMSO), 98% H_2SO_4, 30% H_2O_2, polyethyleneimine solution (PEI, ~50% in H_2O, Mw: ~25,000) and $KMnO_4$ were purchased from Shanghai Chenyun Chemical and Engineering Company (China). Deionized water (>18 MΩ) was produced by an Ultrapure water system (Pall, USA).

The colorimetric measurements of the catalytic activities of enzymes and mimics were performed with a microplate reader (Infinite M200 PRO, Tecan, Austria) and 96-well plates (JET BIOFIL, Guangzhou, China). Transmission electron microscopy (TEM, FEI Tecnai G20, USA) and UV-3600 spectrophotometer (Shimadzu, Japan) were utilized for the characterization of the prepared materials.

2.2. Preparation of PEI-rGO

Typically, according to the modified Hummer's method [53], 98% H_2SO_4 (23 mL) was slowly added into the expandable graphite (0.5 g) with continuous magnetic stirring at 0 °C for 2 h. Subsequently, $KMnO_4$ (3.5 g) was gradually added into the above mixture under stirring. Then, the reaction vessel was allowed to stir at 35 °C for 4 h, after which water (46 mL) was injected gently. The above system was cultured for 40 min at 98 °C, followed by the addition of water (150 mL). Then the mixture was cooled down to room temperature naturally. Furthermore, 98% H_2O_2 was dropped into the mixture until the solution became golden. In addition, the above reaction solution was filtered with a 0.45 μm filter and washed repeatedly with water until the final pH of the filtrate was 5.0–6.0. The filter cake was collected and dried in a vacuum drier at 60 °C.

Next, the obtained GO (10 mg) was dispersed in water (40 mL) by ultrasonic-dispersion for 2 h. Then, 5 mg/mL of PEI solution (40 mL) was gradually dropped into the GO suspension under vigorous stirring. After 20 min of stirring, 80% of $H_2N \cdot NH_2 \cdot H_2O$ was added into the mixture under agitation and then they reacted at 80 °C for 2 h. After being cooled down to room temperature, the mixture was centrifuged for 10 min at 10000 rpm, followed by washing with water, each for three times. At last, the centrifuged PEI-rGO was suspended newly in ultrapure water for use.

2.3. Preparation of the Hemin-BSA composite

According to the previous report [49], the native hemin derivatized with carboxyl groups was covalently bound onto the protein scaffold of BSA to produce a Hemin-BSA composite. Firstly, 19.17 mg EDC and 17.37 mg NHS were added into 1.0 mg/mL hemin (4 mL) and kept activated for 1 h with gently stirring. Then 40 mg/mL of BSA (4 mL) was injected into the above mixture, followed by the adjustment of pH to 9.0–10.0 by using 0.05 M NaOH under vigorous stirring. Finally, the reaction vessel was allowed to stir at 37 °C for 12 h. The so-obtained Hemin-BSA products was collected to be stored at 4 °C for use.

2.4. Preparation of PEI-rGO-Hemin-BSA and PEI-rGO-Hemin-BSA-GOx

10 mg/mL of PEI-rGO (50 μL) was first dispersed into the Hemin-BSA composite (500 μL) under sonication for 4 h. Then PEI-rGO-Hemin-BSA could be obtained by centrifugation (10000 rpm, 10 min), followed by washing with water for three times.

The obtained PEI-rGO-Hemin-BSA was incubated with 2.5% of GA solution (500 μL) at 4 °C overnight. The GA functionalized PEI-rGO-Hemin-BSA was centrifuged and washed similarly as before and mixed with GOx solution (5 mg/mL, 500 μL) overnight at 4 °C. In this way, PEI-rGO-Hemin-BSA-GOx could be obtained by centrifugation. The centrifuged PEI-rGO-Hemin-BSA-GOx was suspended newly in water for use. It could be calculated that the amount of Hemin-BSA fixed on PEI-rGO-Hemin-BSA was 0.104 mg/mg and the fixed GOx on PEI-rGO-Hemin-BSA-GOx was 2.94 mg/mg.

2.5. Kinetic measurement and relative activity comparison

The chromogenic substrates consisting of TMB and H_2O_2 with different concentrations were used for the comparison of the peroxidase-like catalysis activity of native hemin, Hemin-BSA and PEI-rGO-Hemin-BSA [54]. The experiments were performed at pH 6.0 (in phosphate and citric acid monohydrate buffer) and 37 °C, which have been optimized beforehand. All of the reaction products were monitored at 652 nm. Moreover, steady state kinetic assays were comparably carried out for native hemin, Hemin-BSA and PEI-rGO-Hemin-BSA (2.0 μg/mL Hemin for each system), where 2.5 mM H_2O_2 or 0.45 mM TMB was used alternatively at a fixed concentration of one substrate while varying concentration of the second substrate. The Lineweaver-Burk plots by the double reciprocal of the Michaelis-Menten equation were thus performed to calculate the Michaelis-Menten constants.

2.6. Colorimetric investigations of the response of PEI-rGO-Hemin-BSA-GOx to glucose

The response activity of PEI-rGO-Hemin-BSA-GOx was investigated by colorimetric tests with the glucose-TMB substrate. Herein, rGO, PEI-rGO, Hemin-BSA, GOx, and the mixture of Hemin-BSA and GOx with the same concentrations were used as controls. Firstly, the glucose-TMB substrate was prepared as followed, TMB (25 mg) was added into the 5 mL of dimethyl sulfoxide (DMSO) to form solution A. $NaH_2PO_4 \cdot 2H_2O$ (0.368 g) and citric acid monohydrate (0.102 g) were added into water (10 mL) to form solution B. Solution C was formed with the glucose solution of 1 M, the solution A and B (1:1:10, volume ratio). Then, the controls and samples with the same volume were added into 96-well plates respectively. Simultaneously, 200 μL of solution C was added into the above 96-well plates respectively. Absorbance was measured at 652 nm using the microplate reader 20 min later.

Furthermore, different glucose-TMB substrates were prepared with different glucose amounts (0.01–1.50 mM) to investigate the response limit of the system. To investigate the selectivity of PEI-rGO-Hemin-BSA-GOx, its response to DA, AA and UA was studied under the same conditions.

2.7. The activity of PEI-rGO-Hemin-BSA-COx, PEI-rGO-Hemin-BSA-LOx, PEI-rGO-Hemin-BSA-ChOx

The preparation of PEI-rGO-Hemin-BSA-COx, PEI-rGO-Hemin-BSA-LOx, or PEI-rGO-Hemin-BSA-ChOx was performed in the same way as that of PEI-rGO-Hemin-BSA-GOx. The activity of PEI-rGO-Hemin-BSA-COx, PEI-rGO-Hemin-BSA-LOx, and PEI-rGO-Hemin-BSA-ChOx was investigated by colorimetric tests with the cholesterol-TMB substrate, lactate-TMB substrate and choline-TMB substrate, respectively. The cholesterol-TMB substrate was prepared by the dissolution of cholesterol in Triton followed by mild heating due to the limited dissolution of cholesterol in water at ambient temperature. To investigate their response behavior, the cholesterol-TMB, lactate-TMB and choline-TMB substrates were prepared with different cholesterol concentration, lactate
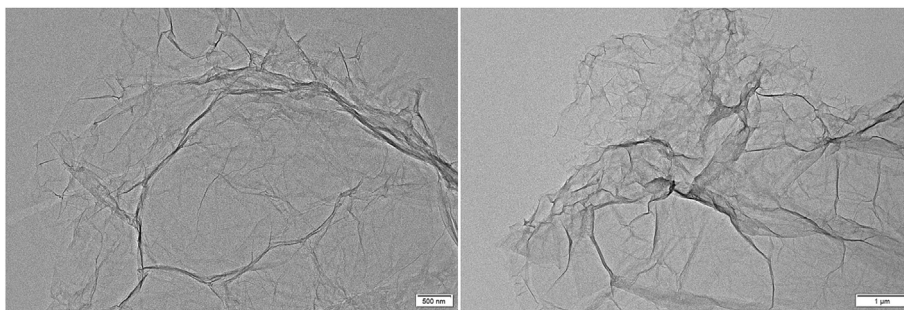
Fig. 1. TEM images of PEI-rGO with different magnifications.

concentration and choline concentration, respectively. The measurement details were similar with that of the PEI-rGO-Hemin-BSA-GOx.

3. Results and discussion

3.1. Characterization of PEI-rGO-Hemin-BSA

Firstly, as stated before, the PEI-rGO was fabricated during a covalent grafting process of PEI to the grapheme sheets. The obtained nanosheets were observed and analyzed using TEM, and the image is shown in Fig. 1. Obviously, large graphene nanosheets are observed folding to form wrinkles. The transparent regions are likely to be monolayer graphene nanosheets. Simultaneously, the formation of PEI-rGO was confirmed by SEM elemental mapping analysis (Fig. 2). Energy disperse spectra (EDS) shows the distribution of C, O, N in the PEI-rGO and rGO, in which the results of rGO are shown as controls. The obvious distribution of N provides the proof of the formation of PEI-rGO. Importantly, surface charges can also prove the formation of PEI-rGO in that the zeta-potential changes from −29.8 mV of rGO to 33.6 mV of PEI-rGO.

With active amino groups in the molecular backbone and relatively high zeta-potential, the PEI-rGO suspension shows such excellent dispersability that there is no precipitation within 24 h. This will be essential for the fabrication of the following stable nanoenzyme dispersion.

Then, the PEI functionalized rGO was further combined with Hemin-BSA, in which Hemin-BSA was formed beforehand with hemin and BSA using EDC/NHS chemical crosslinking. The formation of PEI-rGO-Hemin-BSA composite was confirmed by UV–vis absorption spectra (Fig. 3). There is an absorption peak at 266 nm
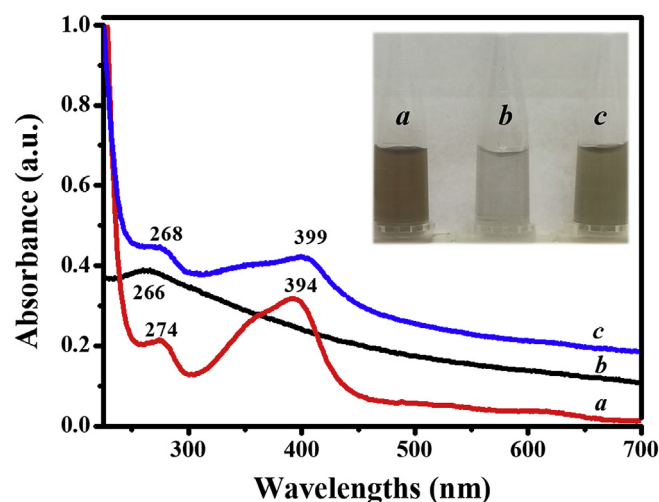

Fig. 3. UV–vis spectra of (a) Hemin-BSA, (b) PEI-rGO, and (c) PEI-rGO-Hemin-BSA.

for the PEI-rGO mainly due to the π-π^* transition of C=C bond [55], while for Hemin-BSA, there are two peaks at 394 nm and 274 nm, corresponding to the absorption of hemin and BSA, respectively. For the developed PEI-rGO-Hemin-BSA composite, the peaks at 399 nm and 268 nm present the component of PEI-rGO and Hemin-BSA. The wavelength shift (from 394 nm to 399 nm, from 274 nm to 268 nm) may be caused by the existence of the π-π interaction of PEI-rGO and Hemin-BSA [43].
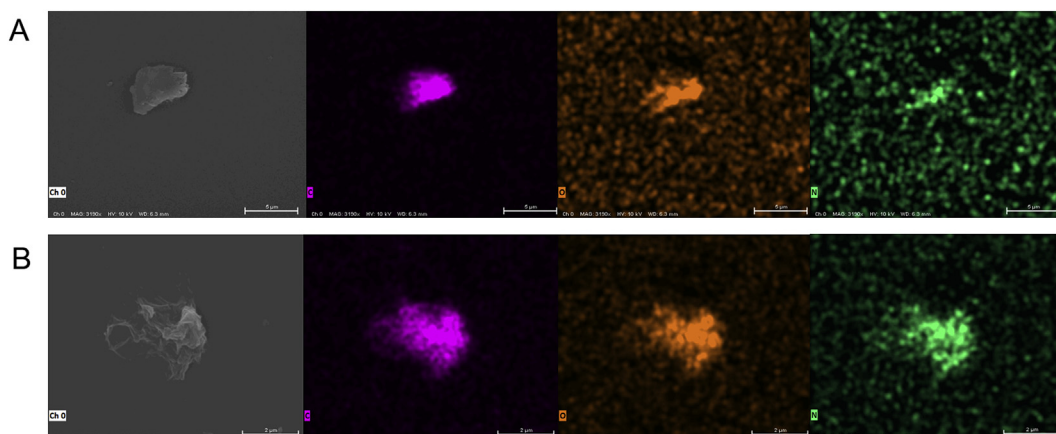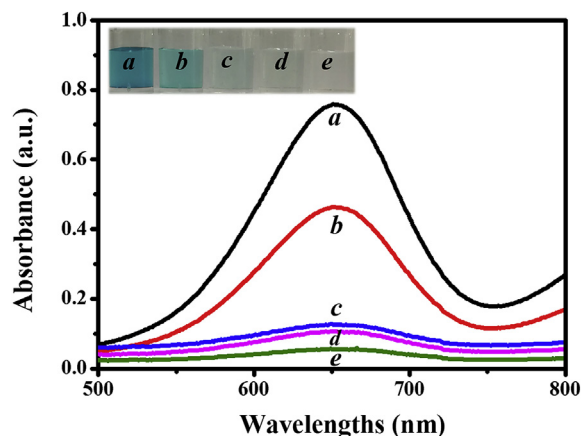

Fig. 2. SEM images of rGO (A) and PEI-rGO (B), and the corresponding energy disperse spectroscopy (EDS) images.

Fig. 4. Absorption spectra and images of 0.4 mM TMB and 10 mM H_2O_2 in the presence of (a) 2.5 μg/mL PEI-rGO-Hemin-BSA; (b) 0.25 μg/mL Hemin-BSA; (c) 2.5 μg/mL PEI-rGO; (d) 2.5 μg/mL rGO; (e) blank at 37 °C in phosphate and citric acid monohydrate buffer (pH 6.0).

3.2. Peroxidase-like activity of PEI-rGO-Hemin-BSA

The peroxidase-like activity of PEI-rGO-Hemin-BSA was investigated by testing the catalysis of the peroxidase substate TMB in the presence of H_2O_2 [49,50]. The catalytic activity of PEI-rGO-Hemin-BSA shows both pH value-dependent and temperature-dependent characteristics (Fig. S1). The highest activity is presented at pH 6.0 and 37 °C, which is consistent with the catalytic conditions of most natural enzymes. As shown in Fig. 4, the PEI-rGO-Hemin-BSA nanocomposite can catalyze the oxidation of TMB by H_2O_2 to produce a typical blue color reaction, whose characterization absorption is located at 652 nm. In contrast, TMB solution in the presence of only H_2O_2 remained colorless within the duration of the experiment, indicating that the oxidation reaction does not happen in the absence of catalyst. Meanwhile, the reaction of rGO, PEI-rGO and Hemin-BSA with H_2O_2 and TMB were used as controls, respectively. Obviously, the color in the PEI-rGO-Hemin-BSA system is much darker than that of Hemin-BSA. Hemin-BSA has been reported to show a higher peroxidase-like activity than native hemin [49]. Therefore, the PEI-rGO-Hemin-BSA composite exhibits a much higher activity.

3.3. Kinetic analysis of the PEI-rGO-Hemin-BSA nanocomposties

The catalytic properties of the nanocomposite was further investigated using steady-state kinetics to get its reacting mechanism as a mimetic enzyme. According to the standard method [56],

kinetic data could be obtained by varying one substrate concentration while keeping the other substrate concentration constant. For example, for the present PEI-rGO-Hemin-BSA nanocomposite, typical Michaelis-Menten curves were obtained with both H_2O_2 (Fig. 5A) and TMB (Fig. 5B) as substrates in a certain range of concentrations. The lineweaver-Burk plot method was used to calculate the Michaelis-Menten constant based on the following equation [56].

$$\frac{1}{v} = \left(\frac{K_m}{V_{max}}\right)\left(\frac{1}{[S]}\right) + \left(\frac{1}{V_{max}}\right)$$

where v is the initial reaction velocity, [S] is the concentration of the substrate, K_m is the M-M constant, V_{max} is the maximum reaction velocity.

The obtained K_m constants and V_{max} values for the PEI-rGO-Hemin-BSA nanocomposites were listed in Table 1, together with those of Hem, Hemin-BSA, HRP for comparison. It is clear that the Km value of the nanocomposites with H_2O_2 as the substrate is lower than that of HRP, while with TMB as the substrate, the value becomes higher than that of HRP. As is well known, Km is an indicator of enzyme affinity for the substrate. These results indicate that the nanocomposites possess a higher affinity for TMB and a lower affinity for H_2O_2 than HRP. In comparison with the reported Hem and Hemin-BSA, the developed nanocomposites show the lowest value both with H_2O_2 as the substrate and with TMB as the substrate, demonstrating that the composites have the highest affinity for TMB and H_2O_2 than Hem and Hemin-BSA. The same conclusion could be obtained with the V_{max} values. This may be contributed to the synergistic effects between rGO and Hemin-BSA, in which the presence of highly delocalized π electrons on the rGO facilitate electrons transfer between the rGO sheets and Hemin-BSA [57].

Table 1
Comparison of K_m and V_{max} among Hemin, Hemin-BSA, and PEI-rGO-Hem-BSA with the reaction substrates of TMB and H_2O_2.

Mimetic Enzymes	Substrates	Km (mM)	$V_{max} \times 10^{-8}$ (M·s^{-1})
Hemin	TMB	4.26 (4.81[49])	1.108 (0.917[50])
Hemin-BSA	TMB	3.02 (2.97[49])	3.914
PEI-rGO-Hemin-BSA	TMB	1.80	8.451
HRP	TMB	0.434[37]	10.00[41]
Hemin	H_2O_2	2.95 (2.85[49])	0.637(0.708[50])
Hemin-BSA	H_2O_2	2.52 (2.46[49])	1.091
PEI-rGO-Hemin-BSA	H_2O_2	2.13	2.339
HRP	H_2O_2	3.70[37]	8.710[50]
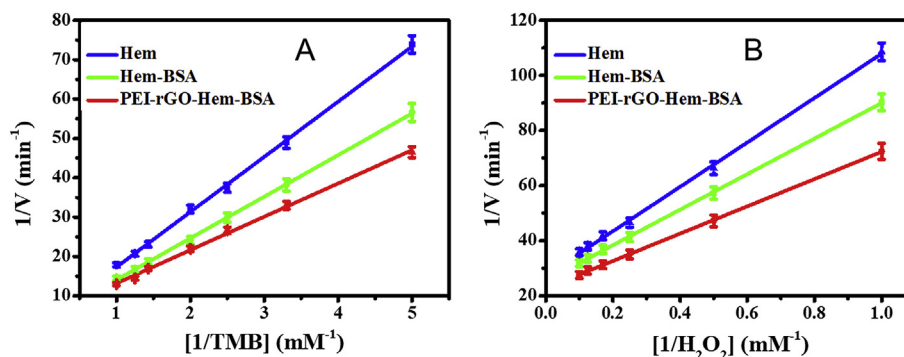
Fig. 5. Double-reciprocal plots for comparison of catalysis activities among Hemin, Hemin-BSA and PEI-rGO-Hemin-BSA by using (A) various TMB concentrations at fixed 2.5 mM H_2O_2 and (B) various H_2O_2 concentrations at fixed 0.45 mM TMB.
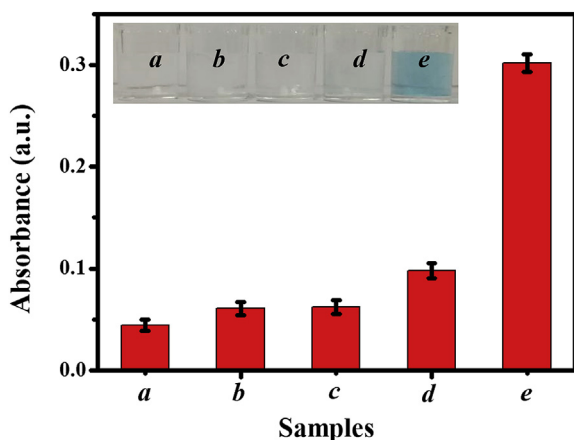
Fig. 6. Comparison of catalysis activities among (a) GOx, (b) Hemin-BSA, (c) the mixture of Hem-BSA and GOx, (d) PEI-rGO and (e) PEI-rGO-Hemin-BSA-GOx in catalyzing the TMB-glucose reactions, together with the corresponding photographs.

3.4. Analytical applications in the determination of small molecules metabolite

It can be expected that when an oxidase is combined with the peroxidase mimic, the prepared PEI-rGO-Hemin-BSA, the corresponding oxidase substrate can be detected. Herein, an integrated nanocomposite was developed by crosslinking GOx with the PEI-rGO-Hemin-BSA nanocomposite using GA as a crosslinker.

The response of the obtained PEI-rGO-Hemin-BSA-GOx toward glucose was investigated using glucose and TMB as the substrates using PEI-rGO, Hemin-BSA, GOx and the mixture of Hemin-BSA and GOx as controls. It can be easily seen from Fig. 6 that the quantitative absorbance of the nanocomposite system at 652 nm is much higher than any of the other studied systems, indicating that its catalytic activity of glucose oxidation is the highest among all the studied systems. Furthermore, the standard curve of the glucose response was obtained. As shown in Fig. 7, adding glucose of various concentrations (containing equal TMB) into the PEI-rGO-Hemin-BSA-GOx dispersion causes the increase of the absorbance at 652 nm to different extents. The linear response of the absorbance versus the glucose concentration 0.03−1.0 mM ($R^2 = 0.99888$) with a detection limit of 0.01 μM. According to previous reports (Table 2), the developed PEI-rGO-Hemin-BSA-GOx is superior to some nanocomposites with catalytic activity in wider linear range and lower
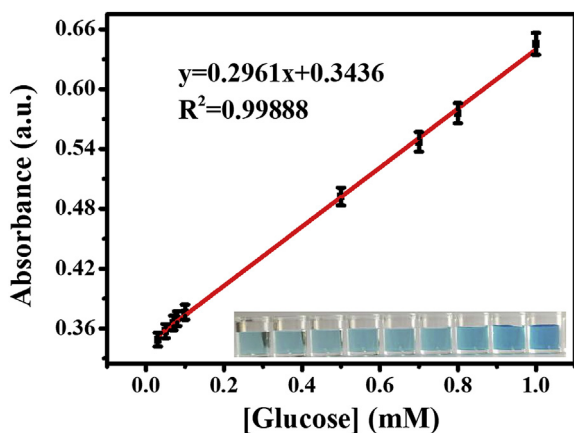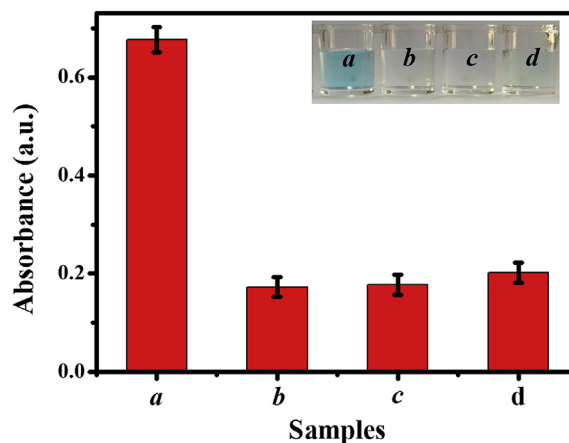
Table 2
The analytical performance of the PEI-rGO-Hemin-BSA-GOx compared with others reported.

Mimetic Enzymes	Detection Limit(μM)	Linear response(mM)	Reference
GO/AuNPs	0.4728	0.002−0.03	[57]
H_2TCPP-NiO	20	0.05−0.5	[58]
Au−Ni/g-C_3N_4	1.7	0.0005−0.03	[59]
VS_2	1.5	0.005−0.2	[60]
PEI-rGO-Hem-BSA	0.01	0.03−1.0	This work

Fig. 8. Colorimetric investigations of the selectivity of the PEI-rGO-Hem-BSA-GOx to (a) 1 mM glucose, (b) 1 mM dopamine (DA), (c) 1 mM ascorbic acid (AA) and (d) 1 mM uric acid (UA), with the corresponding photographs.

detection limit.

The selectivity of PEI-rGO-Hemin-BSA-GOx was further studied using DA, AA and UA as controls under the same conditions. There is a clear color change showing blue when adding glucose (1 mM) (containing TMB) into the dispersion of PEI-rGO-Hemin-BSA-GOX, but no detectable absorbance at 652 nm in Fig. 8 with the addition of DA (1 mM), AA (1 mM) or UA (1 mM) into the same dispersion, indicating that the present system possesses a high selectivity for glucose.

Similarly, when combining COx, the PEI-rGO-Hemin-BSA-COx could be obtained and it can detect cholesterol at a concentration as low as 0.5 μM with a linear response from 0.01 to 0.1 mM, while for PEI-rGO-Hemin-BSA-LOx and PEI-rGO-Hemin-BSA-ChOx, there is a linear response for lactate from 0.05 to 1 mM with a detection limit of 0.1 μM, and choline from 0.1 to 1 mM with a detection limit of 0.01 μM, respectively (Fig. 9). Thus, the present PEI-rGO-Hemin-BSA nanocomposite can be applied to analyze metabolite such as glucose, cholesterol, lactate, choline in a simple and mild way. It will be a promising candidate in clinic for metabolite analysis.

4. Conclusion

In this study, PEI-rGO-Hemin-BSA nanocomposites were prepared by blending PEI-rGO with Hemin-BSA via π-π interactions. The obtained nanocomposites exhibited high peroxidase-like activity by catalyzing H_2O_2 oxidation sensitively and rapidly. Also, the developed enzyme mimics demonstrated the ease of preparation, low cost, high stability and selectivity. Moreover, the nanocomposites could further bind with oxidases conveniently such as GOx, COx, LOx, and ChOx. Thus, their corresponding substrate including glucose, cholesterol, lactate, choline could be detected easily by naked eyes in tiny sample consumption, which provides a
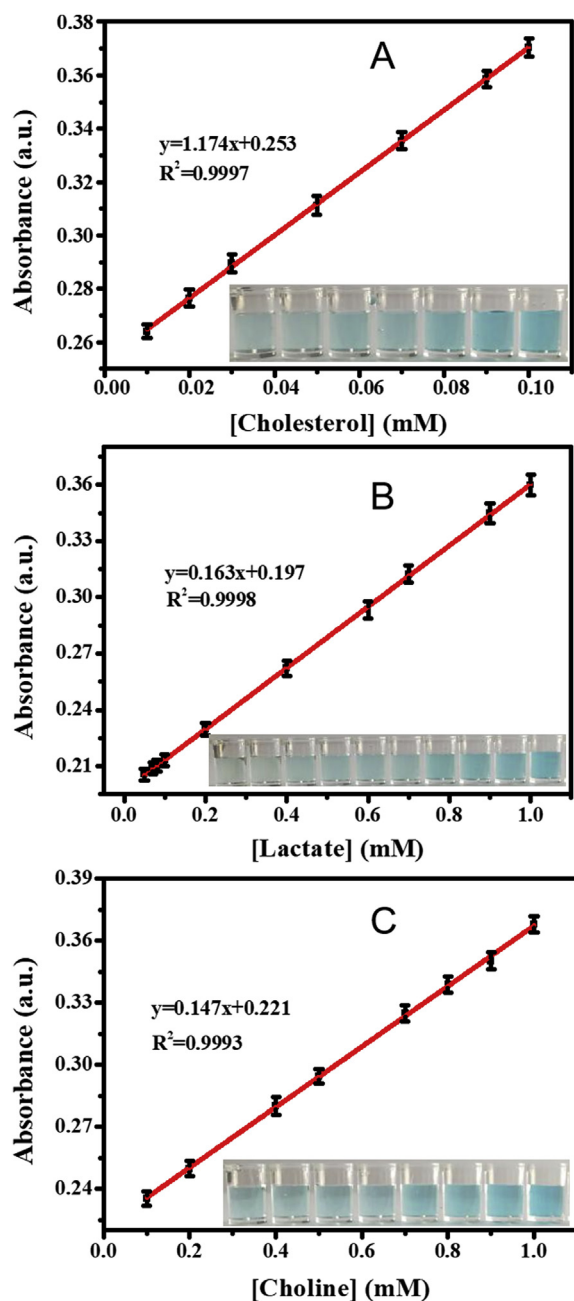

Fig. 7. The linear calibration plot for glucose. The inset image is the colorimetric photos of glucose solution from 0.03 to 1.0 mM.

y=0.2961x+0.3436
R^2=0.99888

Fig. 9. The linear calibration plots of PEI-rGO-Hemin-BSA-COx, PEI-rGO-Hemin-BSA-LOx, PEI-rGO-Hemin-BSA-ChOx for cholesterol, ʟ-lactate, and choline, respectively.

possibility of analyzing multiple metabolites in blood or other biofluids. It could be expected that this efficient strategy will find a wide and important application in clinical diagnosis, healthcare, and management of metabolic disorders and the associated diseases.

Declaration of interest statement

The authors report no conflicts of interest in this work.

Acknowledgements

Appendix A. Supplementary data

Supplementary data to this article can be found online at https://doi.org/10.1016/j.aca.2019.04.028.

References

[1] J.-C. Chou, S.-J. Yan, Y.-H. Liao, C.-H. Lai, Y.-X. Wu, C.-Y. Wu, Remote detection for glucose and lactate based on flexible sensor array, IEEE Sens. J. 18 (2018) 3467–3474.

[2] M. Chung, Y.J. Jang, M.I. Kim, Convenient colorimetric detection of cholesterol using multi-enzyme co-incorporated organic-inorganic hybrid nanoflowers, J. Nanosci. Nanotechnol. 18 (2018) 6555–6561.

[3] H. Liu, X. Li, M. Wang, X. Chen, X. Su, A redox-modulated fluorescent strategy for the highly sensitive detection of metabolites by using graphene quantum dots, Anal. Chim. Acta 990 (2017) 150–156.

[4] J. Li, T. Liu, S. Liu, J. Li, G. Huang, H.H. Yang, Bifunctional magnetic nanoparticles for efficient cholesterol detection and elimination via host-guest chemistry in real samples, Biosens. Bioelectron. 120 (2018) 137–143.

[5] P. Bollella, S. Sharma, A.E.G. Cass, R. Antiochia, Microneedle-based biosensor for minimally-invasive lactate detection, Biosens. Bioelectron. 123 (2019) 152–159.

[6] F. Xie, X. Cao, F. Qu, A.M. Asiri, X. Sun, Cobalt nitride nanowire array as an efficient electrochemical sensor for glucose and H_2O_2 detection, Sens. Actuators, B 255 (2018) 1254–1261.

[7] J. Yuan, Y. Cen, X.J. Kong, S. Wu, C.L. Liu, R.Q. Yu, X. Chu, MnO_2-nanosheet-modified upconversion nanosystem for sensitive turn-on fluorescence detection of H_2O_2 and glucose in blood, ACS Appl. Mater. Interfaces 7 (2015) 10548–10555.

[8] Q. Liu, Y. Yang, X. Lv, Y. Ding, Y. Zhang, J. Jing, C. Xu, One-step synthesis of uniform nanoparticles of porphyrin functionalized ceria with promising peroxidase mimetics for H_2O_2 and glucose colorimetric detection, Sens. Actuators, B 240 (2017) 726–734.

[9] F. Yang, X. Jiang, X. Zhong, S. Wei, R. Yuan, Highly sensitive electrochemiluminescence detection of mucin1 based on V_2O_5 nanospheres as peroxidase mimetics to catalyze H_2O_2 for signal amplification, Sens. Actuators, B 265 (2018) 126–133.

[10] J. Guo, Y. Wang, M. Zhao, 3D flower-like ferrous(II) phosphate nanostructures as peroxidase mimetics for sensitive colorimetric detection of hydrogen peroxide and glucose at nanomolar level, Talanta 182 (2018) 230–240.

[11] M. Chi, Y. Zhu, L. Jing, C. Wang, X. Lu, Fabrication of ternary MoS_2-polypyrrole-Pd nanotubes as peroxidase mimics with a synergistic effect and their sensitive colorimetric detection of l-cysteine, Anal. Chim. Acta 1035 (2018) 146–153.

[12] J. Yao, T. Wu, Y. Sun, Z. Ma, M. Liu, Y. Zhang, S. Yao, A novel biomimetic nanoenzyme based on ferrocene derivative polymer NPs coated with polydopamine, Talanta 195 (2019) 265–271.

[13] X. Wang, Y. Hu, H. Wei, Nanozymes in bionanotechnology: from sensing to therapeutics and beyond, Inorg. Chem. Front. 3 (2016) 41–60.

[14] H. Wei, E. Wang, Nanomaterials with enzyme-like characteristics (nanozymes): next-generation artificial enzymes, Chem. Soc. Rev. 42 (2013) 6060–6093.

[15] K. Chuah, L.M. Lai, I.Y. Goon, S.G. Parker, R. Amal, J. Justin Gooding, Ultra-sensitive electrochemical detection of prostate-specific antigen (PSA) using gold-coated magnetic nanoparticles as 'dispersible electrodes, Chem. Commun. 48 (2012) 3503–3505.

[16] S. Luo, Y. Liu, H. Rao, Y. Wang, X. Wang, Fluorescence and magnetic nanocomposite $Fe_3O_4@SiO_2@Au$ MNPs as peroxidase mimetics for glucose detection, Anal. Biochem. 538 (2017) 26–33.

[17] A. Majouga, M. Sokolsky-Papkov, A. Kuznetsov, D. Lebedev, M. Efremova, E. Beloglazkina, P. Rudakovskaya, M. Veselov, N. Zyk, Y. Golovin, N. Klyachko, A. Kabanov, Enzyme-functionalized gold-coated magnetite nanoparticles as novel hybrid nanomaterials: synthesis, purification and control of enzyme function by low-frequency magnetic field, Colloids Surf., B 125 (2015) 104–109.

[18] J. Liu, L. Meng, Z. Fei, P.J. Dyson, X. Jing, X. Liu, MnO_2 nanosheets as an artificial enzyme to mimic oxidase for rapid and sensitive detection of glutathione, Biosens. Bioelectron. 90 (2017) 69–74.

[19] D. Jampaiah, T.S. Reddy, V.E. Coyle, A. Nafady, S.K. Bhargava, $Co_3O_4@CeO_2$ hybrid flower-like microspheres: a strong synergistic peroxidase-mimicking artificial enzyme with high sensitivity for glucose detection, J. Mater. Chem. B 5 (2016) 720–730.

[20] J. Chen, H. Meng, Y. Tian, R. Yang, Y. Lin, Recent advances in functionalized MnO_2 nanosheets for biosensing and biomedicine applications, Nanoscale Horiz. 4 (2018) 321.

[21] S. Zhu, C. Lei, J. Sun, X.-E. Zhao, X. Wang, X. Yan, W. Liu, H. Wang, Probing NAD+/NADH-dependent biocatalytic transformations based on oxidase mimics of MnO_2, Sens. Actuators, B 282 (2019) 896–903.

[22] W.-H. Chen, M. Vázquez-González, A. Zoabi, R. Abu-Reziq, I. Willner, Biocatalytic cascades driven by enzymes encapsulated in metal-organic framework nanoparticles, Nat. Catal. 1 (2018) 689–695.

[23] W. Xu, X. Zhou, J. Gao, S. Xue, J. Zhao, Label-free and enzyme-free strategy for sensitive electrochemical lead aptasensor by using metal-organic frameworks

loaded with AgPt nanoparticles as signal probes and electrocatalytic enhancers, Electrochim. Acta 251 (2017) 25–31.

[24] C.W. Lien, Y.C. Chen, H.T. Chang, C.C. Huang, Logical regulation of the enzyme-like activity of gold nanoparticles by using heavy metal ions, Nanoscale 5 (2013) 8227–8234.

[25] Y. Hu, H. Cheng, X. Zhao, J. Wu, F. Muhammad, S. Lin, J. He, L. Zhou, C. Zhang, Y. Deng, P. Wang, Z. Zhou, S. Nie, H. Wei, Surface-enhanced Raman scattering active gold nanoparticles with enzyme-mimicking activities for measuring glucose and lactate in living tissues, ACS Nano 11 (2017) 5558–5566.

[26] X.R. Song, N. Goswami, H.H. Yang, J. Xie, Functionalization of metal nano-clusters for biomedical applications, Analyst 141 (2016) 3126–3140.

[27] Y. Tao, M. Li, J. Ren, X. Qu, Metal nanoclusters: novel probes for diagnostic and therapeutic applications, Chem. Soc. Rev. 44 (2015) 8636–8663.

[28] X. Xia, Y. Long, J. Wang, Glucose oxidase-functionalized fluorescent gold nanoclusters as probes for glucose, Anal. Chim. Acta 772 (2013) 81–86.

[29] H. Cheng, Y. Liu, Y. Hu, Y. Ding, S. Lin, W. Cao, Q. Wang, J. Wu, F. Muhammad, X. Zhao, D. Zhao, Z. Li, H. Xing, H. Wei, Monitoring of heparin activity in live rats using metal-organic framework nanosheets as peroxidase mimics, Anal. Chem. 89 (2017) 11552–11559.

[30] L. Zhang, E. Wang, Metal nanoclusters: new fluorescent probes for sensors and bioimaging, Nano Today 9 (2014) 132–157.

[31] L. Yan, F. Zhao, S. Li, Z. Hu, Y. Zhao, Low-toxic and safe nanomaterials by surface-chemical design, carbon nanotubes, fullerenes, metallofullerenes, and graphenes, Nanoscale 3 (2011) 362–382.

[32] L. Wang, Y. Zhang, A. Wu, G. Wei, Designed graphene-peptide nano-composites for biosensor applications: a review, Anal. Chim. Acta 985 (2017) 24–40.

[33] X. Li, Y. Tang, J. Song, W. Yang, M. Wang, C. Zhu, W. Zhao, J. Zheng, Y. Lin, Self-supporting activated carbon/carbon nanotube/reduced graphene oxide flexible electrode for high performance supercapacitor, Carbon 129 (2018) 236–244.

[34] H. Wang, S. Li, Y. Si, N. Zhang, Z. Sun, H. Wu, Y. Lin, Platinum nanocatalysts loaded on graphene oxide-dispersed carbon nanotubes with greatly enhanced peroxidase-like catalysis and electrocatalysis activities, Nanoscale 6 (2014) 8107–8116.

[35] E. Davidd, A. Oleinick, I. Svir, G. Valenti, F. Paolucci, C. Amatore, Theory and simulation for optimising electrogenerated chemiluminescence from tris(2,2′-bipyridine)-ruthenium(II)-Doped silica nanoparticles and tripropylamine, ChemElectroChem 4 (2017) 1719–1730.

[36] K. Li, T. Jiao, R. Xing, G. Zou, J. Zhou, L. Zhang, Q. Peng, Fabrication of tunable hierarchical MXene@AuNPs nanocomposites constructed by self-reduction reactions with enhanced catalytic performances, Sci. China Mater. 61 (2018) 728–736.

[37] H.F. Cui, W.W. Wu, M.M. Li, X. Song, Y. Lv, T.T. Zhang, A highly stable acetylcholinesterase biosensor based on chitosan-TiO$_2$-graphene nano-composites for detection of organophosphate pesticides, Biosens. Bioelectron. 99 (2018) 223–229.

[38] L. Zhang, S. Li, M. Dong, Y. Jiang, R. Li, S. Zhang, X. Lv, L. Chen, H. Wang, Reconstituting redox active centers of heme-containing proteins with bio-mineralized gold toward peroxidase mimics with strong intrinsic catalysis and electrocatalysis for H$_2$O$_2$ detection, Biosens. Bioelectron. 87 (2017) 1036–1043.

[39] J. Chen, J. Ge, L. Zhang, Z. Li, L. Qu, Poly(styrene sulfonate) and Pt bifunctionalized graphene nanosheets as an artificial enzyme to construct a colorimetric chemosensor for highly sensitive glucose detection, Sens. Actuators, B 233 (2016) 438–444.

[40] J. Chen, J. Ge, L. Zhang, Z. Li, J. Li, Y. Sun, L. Qu, Reduced graphene oxide nanosheets functionalized with poly(styrene sulfonate) as a peroxidase mimetic in a colorimetric assay for ascorbic acid, Microchim. Acta 183 (2016) 1847–1853.

[41] C. Jing, G. Jia, Z. Lin, Z. Li, S. Zhou, L. Qu, PSS-GN nanocomposites as highly-efficient peroxidase mimic and their application to colorimetric detection of glucose in serum, RSC Adv. 5 (2015) 90400–90407.

[42] L. Gao, J. Zhuang, L. Nie, J. Zhang, Y. Zhang, N. Gu, T. Wang, J. Feng, D. Yang, S. Perrett, X. Yan, Intrinsic peroxidase-like activity of ferromagnetic

[43] G. Yujing, D. Liu, L. Jing, G. Shaojun, W. Erkang, D. Shaojun, Hemin-graphene hybrid nanosheets with intrinsic peroxidase-like activity for label-free colorimetric detection of single-nucleotide polymorphism, ACS Nano 5 (2011) 1282–1290.

[44] H. Song, Y. Ni, S. Kokot, A novel electrochemical biosensor based on the hemin-graphene nano-sheets and gold nano-particles hybrid film for the analysis of hydrogen peroxide, Anal. Chim. Acta 788 (2013) 24–31.

[45] K.Y. Wang, S.J. Bu, C.J. Ju, C.T. Li, Z.Y. Li, Y. Han, C.Y. Ma, C.Y. Wang, Z. Hao, W.S. Liu, J.Y. Wan, Hemin-incorporated nanoflowers as enzyme mimics for colorimetric detection of foodborne pathogenic bacteria, Bioorg. Med. Chem. Lett 28 (2018) 3802–3807.

[46] D. Cheng, X. Xiao, X. Li, C. Wang, Y. Liang, Z. Yu, C. Jin, N. Zhou, M. Chen, Y. Dong, Y. Lin, Z. Xie, C. Zhang, A non-enzymatic electrochemical sensing platform based on Hemin@MOF composites for detecting hydrogen peroxide and DNA, J. Electrochem. Soc. 165 (2018) B885–B892.

[47] X. Zhou, S. Guo, J. Gao, J. Zhao, S. Xue, W. Xu, Glucose oxidase-initiated cascade catalysis for sensitive impedimetric aptasensor based on metal-organic frameworks functionalized with Pt nanoparticles and hemin/G-quadruplex as mimicking peroxidases, Biosens. Bioelectron. 98 (2017) 83–90.

[48] S. Kumar, P. Bhushan, S. Bhattacharya, Facile synthesis of Au@Ag–hemin decorated reduced graphene oxide sheets: a novel peroxidase mimetic for ultrasensitive colorimetric detection of hydrogen peroxide and glucose, RSC Adv. 7 (2017) 37568–37577.

[49] M. Dong, L. Zhang, R. Li, S. Li, Y. Jiang, Y. Qiao, Z. Duan, R. Li, Q. Wang, H. Wang, Crosslinking catalysis-active center of hemin on the protein scaffold toward peroxidase mimic with powerful catalysis, RSC Adv. 6 (2016) 47595–47599.

[50] S. Li, L. Zhang, Y. Jiang, S. Zhu, X. Lv, Z. Duan, H. Wang, In-site encapsulating gold "nanowires" into hemin-coupled protein scaffolds through biomimetic assembly towards the nanocomposites with strong catalysis, electrocatalysis, and fluorescence properties, Nanoscale 9 (2017) 16005–16011.

[51] C. Shan, L. Wang, D. Han, F. Li, Q. Zhang, X. Zhang, L. Niu, Polyethyleneimine-functionalized graphene and its layer-by-layer assembly with Prussian blue, Thin Solid Films 534 (2013) 572–576.

[52] M.P. Chatrathi, J. Wang, G.E. Collins, Sandwich electrochemical immunoassay for the detection of Staphylococcal enterotoxin B based on immobilized thiolated antibodies, Biosens. Bioelectron. 22 (2007) 2932–2938.

[53] W.S.H. Jr, R.E. Offeman, Preparation of graphitic oxide, J. Am. Chem. Soc. 80 (1958) 1339.

[54] C. Lei, X.E. Zhao, J. Sun, X. Yan, Y. Gao, H. Gao, S. Zhu, H. Wang, A simple and novel colorimetric assay for tyrosinase and inhibitor screening using 3,3',5,5'-tetramethylbenzidine as a chromogenic probe, Talanta 175 (2017) 457–462.

[55] X. Lin, S. Zhu, Q. Xia, J. Ma, Y. Fu, An ultrasensitive electrochemiluminescent d-alanine biosensor based on the synergetic catalysis of a hemin-functionalized composite and gold–platinum nanowires, Anal. Methods 10 (2018) 84–90.

[56] S. Zhu, X.E. Zhao, J. You, G. Xu, H. Wang, Carboxylic-group-functionalized single-walled carbon nanohorns as peroxidase mimetics and their application to glucose detection, Analyst 140 (2015) 6398–6403.

[57] D. Song, Y. Yang, T. Zhou, Y. Liu, S. Song, J. Zhang, H. Lu, Z. Zhao, Hybrid hydrogels based on insitu interpenetrating networks graphene oxide (GO) and Au nanoparticles, and its application as peroxidase mimetics for glucose detection, ChemistrySelect 3 (2018) 10259–10264.

[58] Q. Liu, Y. Yang, H. Li, R. Zhu, Q. Shao, S. Yang, J. Xu, NiO nanoparticles modified with 5,10,15,20-tetrakis(4-carboxyl pheyl)-porphyrin: promising peroxidase mimetics for H$_2$O$_2$ and glucose detection, Biosens. Bioelectron. 64 (2015) 147–153.

[59] G. Darabdhara, J. Bordoloi, P. Manna, M.R. Das, Biocompatible bimetallic Au-Ni doped graphitic carbon nitride sheets: a novel peroxidase-mimicking artificial enzyme for rapid and highly sensitive colorimetric detection of glucose, Sens. Actuators, B 285 (2019) 277–290.

[60] L. Huang, W. Zhu, W. Zhang, K. Chen, J. Wang, R. Wang, Q. Yang, N. Hu, Y. Suo, J. Wang, Layered vanadium(IV) disulfide nanosheets as a peroxidase-like nanozyme for colorimetric detection of glucose, Microchim. Acta 185 (2017) 7.